Pergamon

SCIENCE DIRECT®

Bioorganic & Medicinal Chemistry 11 (2003) 1293–1298

BIOORGANIC & MEDICINAL CHEMISTRY

QSAR Studies on Piperazinylalkylisoxazole Analogues Selectively Acting on Dopamine D_3 Receptor by HQSAR and CoMFA

Mi Young Cha, In Young Lee, Joo Hwan Cha, Kyung Il Choi, Yong Seo Cho, Hun Yeong Koh and Ae Nim Pae*

Biochemicals Research Center, Korea Institute of Science and Technology, PO Box 131, Cheongryang, Seoul, 130-650, South Korea

Received 23 October 2002; accepted 28 November 2002

Abstract—QSAR studies for piperazinylalkylisoxazole analogues were conducted by hologram QSAR (HQSAR) and comparative molecular field analysis (CoMFA) to explain the binding affinities of 264 ligands acting on dopamine D_3 receptor. The HQSAR was assessed by r^2 value of 0.917 and cross validated q^2 value of 0.841. In the CoMFA, r^2 is 0.919 and cross validated q^2 is 0.727. The results provide the tools for predicting the affinity of related compounds and guiding the design of new ligands.

Introduction

The discovery of new ligands with affinity and selectivity for the dopamine D_3 and D_4 receptor subtypes is an important area in medicinal chemistry. Classical dopamine D_2 antagonists are effective in treating schizophrenia.[1] However, they cause severe extrapyramidal side effects that are thought to result from the blockade of D_2 receptors in the striatum of the brain. The distribution of the D_3 and D_4 receptors in the limbic areas of the brain suggests that these receptors may be particularly an attractive target for the design of potential selective antipsychotic drugs without causing extrapyramidal side effects.[2] In this work, we have synthesized piperazinylalkylisoxazole analogues with various substituents and alkyl chain lengths through combinatorial method[3] and carried out quantitative structure and activity relationship (QSAR) studies. Correlating the physicochemical properties of compounds to their biological activities is believed to provide a powerful tool in designing new ligands.[4] It hopefully will minimize the number of compounds that synthetic chemists should prepare and the time needed to discover new drug candidates. In this paper, two methods of QSAR were applied, HQSAR and CoMFA. The widely used CoMFA method (3-D QSAR technique) calculates steric and electrostatic properties according to Lennard-Jones and Coulomb potentials. CoMFA analysis involves the alignment of molecules in a structurally reasonable manner on the basis of the assumption that each compound acts via a common binding site. Therefore 3-D structures of 262 compounds with various alkyl chain lengths are hard to align. However, HQSAR, a 2-D-QSAR protocol (Tripos Associates, Inc.), eliminates the need for generation of 3-D structure, putative binding conformations, and molecular alignment. In HQSAR, each molecule in the database is broken down into a series of unique structural fragments, which are arranged to form a molecular hologram. Unlike other fragment-based fingerprinting methods, HQSAR encodes all possible molecular fragments (linear, branched, and overlapping). Supplementary 3-D information, such as hybridization and chirality, may also be encoded in the molecular holograms.

In this study, we carried out a HQSAR study on a total of 262 compounds having various alkyl chain lengths ($n=1$–4) which were synthesized by solution phase combinatorial chemistry and performed CoMFA analysis for the fine tuning on selected a series ($n=4$) which is the most active (Fig. 1).

*Corresponding author. Tel.: +82-2-958-5185; fax: +82-2-958-5189; e-mail: anpae@kist.re.kr

0968-0896/03/$ - see front matter © 2003 Elsevier Science Ltd. All rights reserved.
doi:10.1016/S0968-0896(02)00617-X

Results and Discussion

Structure building

Structures of entire sets of piperazinylalkylisoxazole analogues were built using SYBYL 6.6[5] molecular modeling software. For the HQSAR study, 2-D structures of ligands were generated using CONCORD. The structure energy minimization was performed for CoMFA analysis using the standard Tripos molecular mechanics force field and Gasteiger–Huckel charge, with a 0.005 kcal/mol energy gradient convergence criterion on Silicon Graphics IRIS Indigo II R4000 computer system. Low energy conformation was searched by random conformational search.

Hologram QSAR

HQSAR module of SYBYL 6.6[5] (Tripos Inc.) was used for HQSAR study.[6] A training set having 175 compounds and a test set having 87 compounds were utilized for analysis. The binding affinity (% inhibition value at 1 μM) of ligands on dopamine D_3 receptor was used for dependent column. A number of parameters were adjusted to optimize the HQSAR model by varying fragment type, length and hologram length shown in Table 1. The best model was built using atom, bond, connectivity, donor and acceptor as fragment type, 257 as hologram length and 4–7 as fragment size. The result of correlation of molecular hologram descriptor and binding affinity gave good r^2 value (0.917), cross validated q^2 value (0.841) and included optimum number of component (18) for minimizing of model complexity. The HQSAR actual versus predicted activity for the training set are shown in Table 2 and plotted in Figure 2. In the test set compounds to validate, it gave good predictive power as shown in Table 3 and Figure 3. The binding affinities of ligands are getting improved as increasing chain length from $n=1$ to $n=4$. We carried out the 3-D-CoMFA analysis on the selected series of compounds ($n=4$) which showed the best activities for the fine tuning.

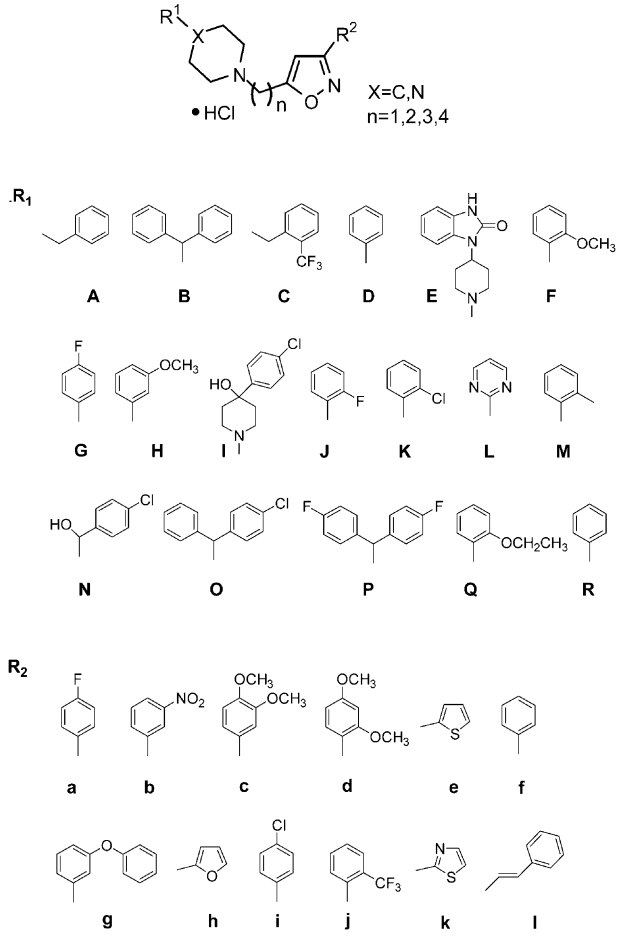

Figure 1. Structure of piperazinylalkylisoxazole analogues used in the QSAR analysis.

CoMFA

CoMFA study was performed using SYBYL 6.6/CoMFA[5] routine. Among 42 compounds having alkyl chain length ($n=4$), 29 compounds were used for a

Table 1. Comparison of HQSAR results according to different options

Hologram length	Fragment size	r^2 (standard error)	q^2 (standard error)	No. of component	Model
307	2-5	0.834 (14.47)	0.767 (17.15)	19	1[a]
281	2-5	0.820 (14.67)	0.760 (16.92)	10	2[b]
343	2-5	0.833 (14.40)	0.764 (17.12)	16	3[c]
319	2-5	0.883 (12.08)	0.828 (14.66)	17	4[d]
319	2-5	0.883 (12.15)	0.828 (14.76)	19	5[e]
375	3-6	0.832 (14.25)	0.770 (16.67)	12	1
401	3-6	0.862 (13.06)	0.794 (15.95)	15	2
413	3-6	0.866 (13.13)	0.803 (15.94)	22	3
375	3-6	0.921 (10.13)	0.841 (14.41)	24	4
413	3-6	0.893 (11.53)	0.827 (14.64)	16	5
257	4-7	0.865 (12.89)	0.797 (15.81)	15	1
236	4-7	0.873 (12.51)	0.805 (15.48)	15	2
281	4-7	0.865 (12.89)	0.801 (15.66)	15	3
257	**4-7**	**0.917 (10.18)**	**0.841 (14.13)**	**18**	**4**
224	4-7	0.925 (9.89)	0.846 (14.18)	24	5
353	5-8	0.865 (12.73)	0.798 (15.58)	11	1
337	5-8	0.900 (11.09)	0.831 (14.15)	15	2
320	5-8	0.894 (11.75)	0.819 (15.30)	23	3
370	5-8	0.940 (8.98)	0.871 (13.21)	29	4
151	5-8	0.934 (9.48)	0.862 (13.71)	30	5

[a]Atoms + bonds.
[b]Atoms + bonds + connections.
[c]Atoms + bonds + connections + hydrogens.
[d]Atoms + bonds + connections + donor and acceptors.
[e]Atoms + bonds + connections + hydrogens + donor and acceptors.

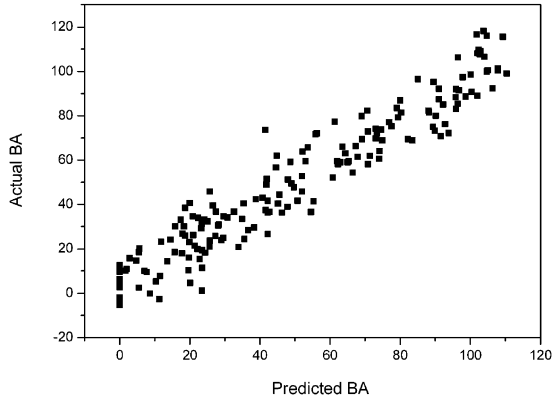

Figure 2. The HQSAR graph of predicted activity versus actual activity data for the training set.

Table 2. Actual and predicted activities of training set by HQSAR

Entry	*n*	R_1	R_2	Actual[a]	Predicted[b]	Residual[c]
1	1	C	c	11.8	23.1	11.3
2	1	I	c	15.7	18.6	2.9
3	1	K	c	29.7	34.7	5.0
4	1	I	i	0.0	−1.9	1.9
5	1	M	i	0.0	9.5	9.5
6	1	A	i	0.0	−2.7	2.7
7	1	E	b	5.6	2.5	3.1
8	1	C	b	8.7	−0.1	8.8
9	1	I	b	0.0	−4.7	4.7
10	1	M	b	0.0	3.5	3.5
11	1	A	b	0.0	−5.5	5.5
12	1	E	e	19.6	10.4	9.2
13	1	C	e	11.6	7.8	3.8
14	1	M	e	23.6	11.4	12.2
15	1	E	d	17.8	17.9	0.1
16	1	C	d	22.8	15.3	7.5
17	1	A	d	1.7	10.0	8.3
18	1	K	d	17.9	26.9	9.0
19	1	B	d	25.8	45.7	19.9
20	1	K	j	23.5	1.2	22.3
21	1	B	j	5.7	20.0	14.3
22	1	E	l	0.0	12.6	12.6
23	1	C	l	7.1	10.0	2.9
24	1	I	l	10.4	5.4	5.0
25	1	A	l	20.1	4.6	15.5
26	1	K	l	24.4	18.2	6.2
27	1	B	l	35.4	40.4	5.0
28	1	E	g	0.0	5.3	5.3
29	1	C	g	0.0	2.7	2.7
30	1	M	g	7.8	9.6	1.8
31	1	A	g	11.3	−2.6	13.9
32	1	K	g	13.6	14.3	0.7
33	2	B	b	44.6	56.6	12.0
34	2	O	b	42.8	36.7	6.1
35	2	A	b	33.9	20.9	13.0
36	2	C	l	42.3	41.6	0.7
37	2	B	l	56.2	72.0	15.8
38	2	O	l	48.7	59.1	10.4
39	2	A	l	42.3	36.3	6.0
40	2	B	g	62.1	59.4	2.7
41	2	A	g	25.8	23.7	2.1
42	2	E	g	76.9	77.0	0.1
43	2	D	c	85.1	96.5	11.4
44	2	B	c	90.2	79.9	10.3
45	2	C	d	50.8	41.7	9.1
46	2	D	d	98.7	88.7	10.0
47	2	B	d	73.3	72.1	1.2
48	2	O	d	60.8	52.1	8.7
49	2	A	d	46.3	36.3	10.0
50	2	E	d	62.9	59.1	3.8
51	2	C	j	19.8	16.0	3.8
52	2	D	j	64.4	63.0	1.4
53	2	A	j	0.0	10.6	10.6
54	2	E	j	34.9	33.4	1.5
55	2	O	i	26.6	39.4	12.8
56	2	D	e	70.6	82.3	11.7
57	2	O	e	52.0	45.8	6.2
58	2	A	e	15.9	30.0	14.1
59	2	E	e	52.0	52.7	0.7
60	3	A	i	5.5	18.5	13.0
61	3	A	b	2.9	15.7	12.8
62	3	A	d	23.4	31.2	7.8
63	3	A	e	29.6	24.8	4.8
64	3	A	k	22.2	20.0	2.2
65	3	A	l	24.2	33.1	8.9
66	3	B	i	66.5	54.2	12.3
67	3	B	b	42.0	51.5	9.5
68	3	B	e	74.1	60.6	13.5
69	3	B	a	70.9	58.2	12.7
70	3	B	f	65.0	59.1	5.9
71	3	C	i	29.1	23.8	5.3
72	3	C	b	25.7	21.1	4.6
73	3	C	c	45.6	44.3	1.3

Table 2 (*continued*)

Entry	*n*	R_1	R_2	Actual[a]	Predicted[b]	Residual[c]
74	3	C	d	54.6	36.5	18.1
75	3	C	l	18.7	38.4	19.7
76	3	D	i	27.5	36.7	9.2
77	3	D	b	22.4	33.9	11.5
78	3	D	a	20.0	40.6	20.6
79	3	D	g	32.6	36.8	4.2
80	3	D	l	48.0	51.3	3.3
81	3	E	i	74.9	68.9	6.0
82	3	E	b	67.3	66.2	1.1
83	3	E	d	88.2	81.6	6.6
84	3	E	e	77.6	75.3	2.3
85	3	E	a	70.9	72.9	2.0
86	3	E	f	74.6	73.8	0.8
87	3	E	g	93.9	72.1	21.8
88	3	E	l	79.1	83.5	4.4
89	3	F	b	71.4	61.8	9.6
90	3	F	c	92.3	85.1	7.2
91	3	F	k	63.5	66.1	2.6
92	3	F	a	62.3	58.1	4.2
93	3	F	f	69.2	69.4	0.2
94	3	F	l	83.5	68.8	14.7
95	4	A	e	53.7	65.6	11.9
96	4	B	a	110.4	99.0	11.4
97	4	B	b	106.4	92.3	14.1
98	4	B	c	109.3	115.5	6.2
99	4	B	d	102.7	107.7	5.0
100	4	B	e	107.8	101.4	6.4
101	4	B	f	104.7	99.9	4.8
102	4	B	g	89.6	95.1	5.5
103	4	B	l	102.4	109.6	7.2
104	4	C	b	44.8	61.9	17.1
105	4	C	d	61.4	77.3	15.9
106	4	C	f	82.3	69.5	12.8
107	4	C	l	79.4	79.2	0.2
108	4	D	b	95.9	83.0	12.9
109	4	D	c	96.5	106.3	9.8
110	4	D	d	100.1	98.5	1.6
111	4	D	e	91.1	92.1	1.0
112	4	D	f	100.4	90.6	9.8
113	4	D	g	102.1	89.0	13.1
114	4	D	l	107.9	100.4	7.5
115	4	E	b	41.5	73.6	32.1
116	4	F	b	105.0	100.5	4.5
117	4	F	d	104.7	116.0	11.3
118	4	F	f	102.1	108.1	6.0
119	4	F	g	104.0	106.5	2.5
120	3	G	i	18.7	26.0	7.3
121	3	G	e	25.2	32.4	7.2
122	3	G	a	18.3	30.0	11.7
123	3	G	f	28.3	30.9	2.6
124	3	G	g	21.0	26.1	5.1
125	3	H	i	36.6	28.3	8.3
126	3	H	c	41.9	48.8	6.9
127	3	H	e	20.9	34.7	13.8
128	3	H	f	17.5	33.2	15.7
129	3	H	l	40.8	42.9	2.1
130	3	J	b	21.5	21.3	0.2
131	3	J	e	30.8	34.1	3.3
132	3	J	g	14.5	24.1	9.6
133	3	J	l	38.8	42.4	3.6
134	3	K	f	23.6	19.3	4.3
135	3	K	g	2.0	10.9	8.9
136	3	K	l	23.3	29.1	5.8
137	3	L	i	27.3	25.7	1.6
138	3	L	b	19.9	23.0	3.1
139	3	L	a	38.4	29.7	8.7
140	3	L	f	28.1	30.6	2.5
141	3	L	l	45.2	40.3	4.9
142	3	N	l	47.9	39.0	8.9
143	3	M	c	42.3	26.6	15.7
144	3	M	f	4.7	14.6	9.9
145	3	M	g	0.0	6.2	6.2

(*continued on next page*)

Table 2 (*continued*)

Entry	*n*	R_1	R_2	Actual[a]	Predicted[b]	Residual[c]
146	3	M	l	35.6	24.4	11.2
147	3	O	i	55.3	41.3	14.0
148	3	O	e	49.7	47.7	2.0
149	3	P	i	65.4	59.4	6.0
150	3	P	c	69.1	79.9	10.8
151	3	P	g	53.0	59.4	6.4
152	3	P	l	73.1	74.0	0.9
153	3	Q	i	80.3	81.4	1.1
154	3	Q	c	96.8	91.5	5.3
155	3	Q	a	89.4	74.9	14.5
156	3	Q	f	88.1	82.2	5.9
157	3	Q	l	96.0	92.0	4.0
158	4	G	a	91.6	70.8	20.8
159	4	G	b	74.2	64.1	10.1
160	4	G	c	91.1	87.3	3.8
161	4	G	e	89.9	73.2	16.7
162	4	H	e	92.8	76.1	16.7
163	4	J	c	96.4	85.3	11.1
164	4	J	f	73.1	69.7	3.4
165	4	L	a	49.0	49.4	0.4
166	4	L	b	52.2	63.8	11.6
167	4	N	e	55.9	71.5	15.6
168	4	M	l	67.9	61.5	6.4
169	4	O	e	95.8	88.5	7.3
170	4	O	f	80.0	86.9	6.9
171	4	O	h	41.7	37.5	4.2
172	4	P	b	97.9	97.4	0.5
173	4	Q	b	102.9	109.1	6.2
174	4	Q	e	103.8	118.2	14.4
175	4	Q	f	101.8	116.6	14.8

[a]Actual binding affinity, binding affinity (% inhibition at 1 μM).
[b]Predicted binding affinity.
[c]|Actual–Predicted | binding affinity.

training set and 13 compounds were utilized as a test set. Using compound 242 (most active compound of the series) as template molecule, superposition of all analogues was performed with common 1-pentyl-4-phenyl piperazine containing in all compounds. Figure 4 shows the results of such alignment.

The CoMFA was used as a descriptor, and the activities for dopamine D_3 receptor was used as a dependent column. Good cross-validated q^2 (0.727) and conventional r^2 (0.919) values by the PLS and CoMFA analysis indicated this method a considerably reliable one for pre-

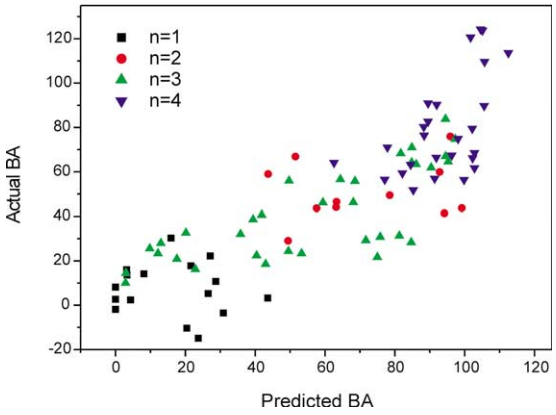

Figure 3. The HQSAR graph of actual activity versus predicted activity data for the test set (black: $n=1$, yellow: $n=2$, green: $n=3$, blue: $n=4$).

Table 3. Actual and predicted activities of test set by HQSAR

Entry	*n*	R_1	R_2	Actual	Predicted	Residual
176	3	O	b	39.4	38.6	0.8
177	3	O	c	90.4	61.8	28.6
178	3	O	f	59.4	46.1	13.3
179	3	O	l	49.7	55.9	6.2
180	3	P	b	64.4	56.6	7.8
181	3	P	a	86.1	63.3	22.8
182	3	P	f	84.8	64.2	20.6
183	3	Q	b	81.7	68.3	13.4
184	3	Q	e	94.5	83.8	10.7
185	4	H	b	91.9	66.4	25.5
186	4	H	c	92.0	90.3	1.7
187	4	J	e	98.1	74.9	23.2
188	4	J	l	102.2	79.4	22.8
189	4	K	e	102.8	61.6	41.2
190	4	K	f	99.8	56.4	43.4
191	4	K	l	102.3	66.2	36.1
192	4	M	c	96.3	67.4	28.9
193	4	M	e	91.4	57.0	34.4
194	4	M	f	85.3	51.7	33.6
195	4	P	c	101.7	120.6	18.9
196	1	A	c	21.6	17.8	3.8
197	1	E	i	26.5	5.2	21.3
198	1	C	i	0.0	2.6	2.6
199	1	K	i	8.1	14.2	6.1
200	1	K	b	0.0	8.2	8.2
201	1	B	b	15.9	30.3	14.4
202	1	I	e	43.6	3.2	40.4
203	1	A	e	4.3	2.4	1.9
204	1	K	e	3.2	16.1	12.9
205	1	I	d	28.7	10.8	17.9
206	1	M	d	27.1	22.2	4.9
207	1	C	j	20.4	−10.4	30.8
208	1	I	j	23.7	−14.9	38.6
209	1	M	j	30.9	−3.5	34.4
210	1	M	l	3.3	13.6	10.3
211	1	I	g	0.0	−1.9	1.9
212	2	E	b	57.6	43.6	14.0
213	2	D	l	99.2	43.7	55.5
214	2	E	l	43.7	59.0	15.3
215	2	C	g	49.4	29.0	20.4
216	2	D	g	94.2	41.4	52.8
217	2	O	g	63.3	46.5	16.8
218	2	C	c	78.5	49.5	29.0
219	2	O	c	92.8	59.9	32.9
220	2	A	c	63.2	44.1	19.1
221	2	E	c	51.5	66.9	15.4
222	2	D	i	95.9	76.0	19.9
223	3	A	a	40.4	22.4	18.0
224	3	A	f	53.3	23.3	30.0
225	3	A	g	43.0	18.6	24.4
226	3	B	c	97.3	74.7	22.6
227	3	B	d	94.5	66.9	27.6
228	3	B	k	68.6	55.7	12.9
229	3	F	i	95.3	64.6	30.7
230	3	F	e	84.9	70.9	14.0
231	4	A	a	84.5	63.2	21.3
232	4	A	b	77.1	56.5	20.6
233	4	A	f	62.6	64.1	1.5
234	4	A	g	82.2	59.3	22.9
235	4	C	a	102.8	68.6	34.2
236	4	C	e	77.9	71.0	6.9
237	4	D	a	105.6	89.7	15.9
238	4	E	a	88.3	80.3	8.0
239	4	E	e	89.5	82.7	6.8
240	4	E	g	88.4	76.4	12.0
241	4	E	l	89.5	90.9	1.4
242	4	F	a	112.5	113.6	1.1
243	4	F	c	105.1	123.8	18.7
244	4	F	e	105.7	109.7	4.0
245	4	F	l	104.6	124.3	19.7
246	3	G	b	12.2	23.3	11.1
247	3	G	l	41.9	40.6	1.3
248	3	H	b	9.8	25.6	15.8

(*continued on next page*)

Table 3 (*continued*)

Entry	*n*	R_1	R_2	Actual	Predicted	Residual
249	3	J	a	13.0	28.0	15.0
250	3	J	f	20.2	32.6	12.4
251	3	K	i	3.0	14.5	11.5
252	3	K	c	81.3	31.3	50.0
253	3	K	e	17.6	20.8	3.2
254	3	L	c	68.1	46.2	21.9
255	3	L	e	35.8	32.1	3.7
256	3	N	i	49.5	24.4	25.1
257	3	N	b	75.0	21.6	53.4
258	3	N	e	75.8	30.7	45.1
259	3	N	a	84.7	28.3	56.4
260	3	N	f	71.7	29.2	42.5
261	3	M	e	22.9	16.2	6.7
262	3	M	a	2.9	10.0	7.1

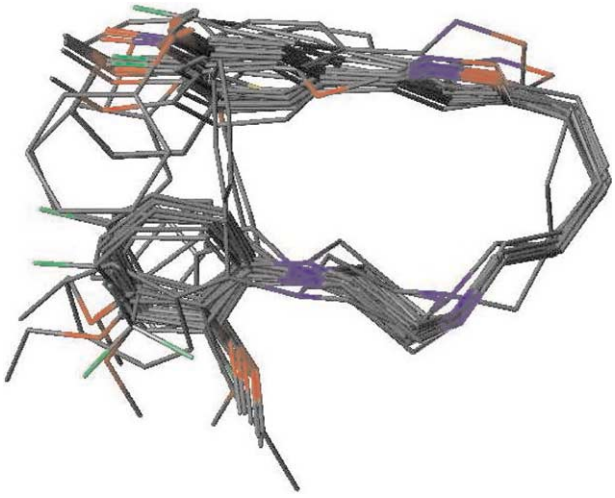

Figure 4. Stereoview of the 29 compounds aligned.

Table 4. Summary of CoMFA-PLS results of the training set

Parameters	Parameters
No. of components	4
Probe atom	C (sp^3, +1)
Cross-validated r^2	0.727
Standard error of estimate	2.541
Conventional r^2	0.919
F values	68.100
Relative steric contribution	0.383
Relative electrostatic contribution	0.617

dicting activities of related structures. The contributions of steric and electrostatic fields were 0.383 and 0.617, respectively.

All of the structures generated were aligned into 3-D lattice box by fitting with isoxazole as a common structure. An sp^3 carbon atom with a +1.0 charge was selected as a probe for the calculation of the steric and electrostatic field. Values of the steric and electrostatic energies were truncated at 30 kcal/mol. For each of the alignment sets, the steric and coulombic energy fields were individually calculated at each lattice interaction of

Table 5. Actual and predicted activities of training set

Entry	*n*	R_1	R_2	CoMFA	Actual	Predicted	Residual
102	4	B	g	240	89.6	87.6	2.0
107	4	C	l	194	79.4	79.3	0.1
108	4	D	b	164	95.9	94.7	1.2
109	4	D	c	176	96.5	95.5	1.1
111	4	D	e	152	91.1	92.9	−1.8
113	4	D	g	164	102.1	104.7	−2.6
114	4	D	l	164	107.9	103.6	4.3
116	4	F	b	172	105.0	105.2	−0.2
117	4	F	d	192	104.7	104.8	−0.1
119	4	F	g	200	104.0	103.6	0.4
158	4	G	a	158	91.6	93.9	−2.3
160	4	G	c	176	91.1	91.7	−0.6
162	4	H	e	170	92.8	91.2	1.6
163	4	J	c	174	96.4	98.1	−1.7
173	4	Q	b	184	102.9	103.2	−0.3
174	4	Q	e	168	103.8	104.2	−0.4
186	4	H	c	186	92.0	92.2	−0.2
188	4	J	l	164	102.2	106.1	−3.9
190	4	K	f	160	99.8	94.6	5.2
191	4	K	l	168	102.3	105.1	−2.8
192	4	M	c	178	96.3	93.5	2.8
193	4	M	e	158	91.4	90.7	0.7
194	4	M	f	160	85.3	90.6	−5.4
231	4	A	a	168	84.5	86.5	−2.0
234	4	A	g	204	82.2	81.9	0.3
242	4	F	a	164	112.5	108.5	4.0
243	4	F	c	180	105.1	104.4	0.7
245	4	F	l	178	104.6	105.2	−0.6
263	4	Q	c	194	103.1	102.6	0.5

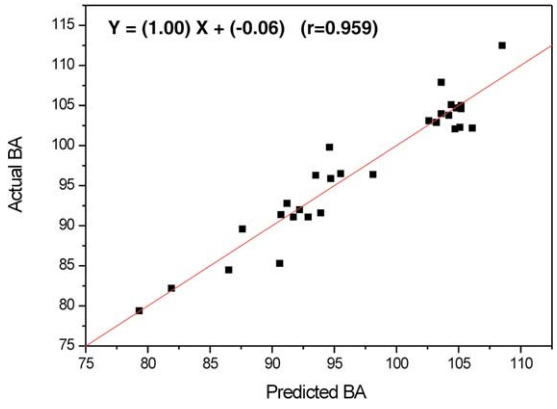

Figure 5. The graph of predicted activity versus actual activity data for the training set.

Table 6. Actual and predicted activities of test set

Entry	*n*	R_1	R_2	CoMFA	Actual	Predicted	Residual
106	4	C	f	178	82.3	72.1	10.2
110	4	D	d	182	100.1	98.2	1.9
112	4	D	f	156	100.4	93.6	6.8
118	4	F	f	188	102.1	92.4	9.7
169	4	O	e	202	95.8	91.1	4.7
172	4	P	b	204	97.9	90.2	7.7
175	4	Q	f	176	101.8	99.6	2.2
185	4	H	b	172	91.9	91.5	0.4
187	4	J	e	152	98.1	95.3	2.8
189	4	K	e	160	102.8	94.5	8.3
237	4	D	a	154	105.6	97.3	8.3
244	4	F	e	166	105.7	94.4	11.4
264	4	K	h	156	97.9	93.5	4.4

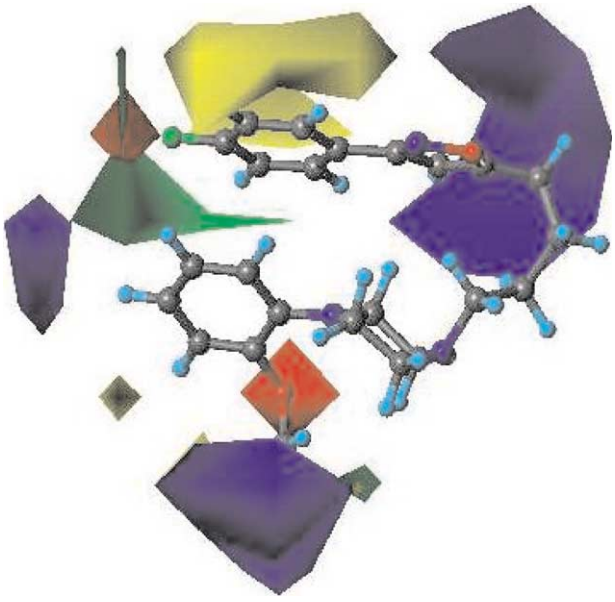

Figure 6. CoMFA contour map and the graph of predicted activity versus actual activity data for the training set. Sterically favored/or disfavored areas are shown in green/or yellow color. Electronegative potential favored/or disfavored areas are depicted in red/or blue.

regularly spaced grid of 2 Å unit in all x, y and z directions. The partial least squares (PLS) method was used for fitting the 3-D structural features and their biological activities.

The results of the CoMFA analysis are summarized in Table 4, and for training set and test set, their actual and predicted activities are shown in Tables 5 and 6. The 3-D QSAR derived from CoMFA showed that binding affinities of the analogues in the training set correlated well with their steric and electrostatic fields. In this case the electrostatic field was the most contributing factor (0.617) for their activities. Figure 5 shows good correlation between actual and predicted activities used as CoMFA trainging set (slope = 1.00, correlation = 0.959).

The major steric and electrostatic features of the QSAR are illustrated in Figure 6 as 3-D solid surfaces. In the steric CoMFA map shown in colors of green and yellow, the green colored part around the substituent group of the molecule indicated that a sterically bulky group at that position could result in the enhancement of the antagonistic activity. In the electrostatic CoMFA map, the red color showed that more electronegative group at that region could confer better activities.

Conclusion

The QSAR studies—hologram QSAR (HQSAR) and comparative molecular field analysis (CoMFA)—for piperazinylalkylisoxazole analogues selectively acting on dopamine D_3 receptor were conducted with data set composed of 264 ligands. The HQSAR for ligands having various alkyl chain length ($n = 1$–4) was run with the options of atoms, connections and donor–acceptors, and it was assessed by r^2 value of 0.917 and cross validated q^2 value of 0.841. The binding affinities of ligands are getting improved as increasing chain length from $n = 1$ to $n = 4$. In CoMFA for ligands having alkyl chain length ($n = 4$), r^2 is 0.919 and cross validated q^2 is 0.727 as well as the contributions of steric and electrostatic fields were 0.383 and 0.617, respectively. The results provide the tools for predicting the affinity of related compounds, and for guiding the design of new ligands having selectivity and activity.

References and Notes

1. Montmayeur, J. P.; Borrelli, E. *Proc. Natl. Acad. Sci.* **1991**, *88*, 3135.
2. Baldessarini, R. J.; Tarsey, D. *Ann. Rev. Neurosci.* **1980**, *3*, 23.
3. Cha, M. Y.; Choi, B. C.; Kang, K. H.; Pae, A. N.; Choi, K. I.; Cho, Y. S.; Koh, H. Y.; Lee, H. Y.; Jung, D.; Kong, J. Y. *Bioorg. Med. Chem. Lett.* **2002**, *12*, 1327.
4. Avery, M. A.; Alvim-Gaston, M.; Rodrigues, C. R.; Barreiro, E. J.; Cohen, F. E.; Sabnis, Y. A.; Woolfrey, J. R. *J. Med. Chem.* **2002**, *45*, 292.
5. *SYBYL version 6.6*; St Louis, Tripos associates, 1998.
6. Pae, A. N.; Kim, S. Y.; Kim, H. Y.; Joo, H. J.; Cho, Y. S.; Choi, K. I.; Choi, J. H.; Koh, H. Y. *Bioorg. Med. Chem. Lett.* **1999**, *9*, 2685.